BIOCHEMISTRY
including biophysical chemistry & molecular biology
Article

Biochemistry **2011,** *50,* 151–161 151
DOI: 10.1021/bi1016155

Energetics of Ligand Recognition and Self-Association of Bovine β-Lactoglobulin: Differences between Variants A and B[†]

Martiniano Bello, María del Carmen Portillo-Téllez, and Enrique García-Hernández*

Instituto de Química, Universidad Nacional Autónoma de México, Circuito Exterior, Ciudad Universitaria, México 04510, D.F., México

Received October 6, 2010; Revised Manuscript Received November 26, 2010

ABSTRACT: An understanding of the interplay between structure and energetics is crucial for the optimization of modern protein engineering techniques. In this context, the study of natural isoforms is a subject of major interest, as it provides the scenario for analyzing mutations that have endured during biological evolution. In this study, we performed a comparative analysis of the ligand-recognition and homodimerization energetics of bovine β-lactoglobulin variants A (βlgA) and B (βlgB). These variants differ by only two amino-acid substitutions: 64th ($Asp_A \rightarrow Gly_B$), which is fully exposed to the solvent, and 118th ($Val_A \rightarrow Ala_B$), immersed in the hydrophobic core of the protein. Calorimetric measurements revealed significant enthalpic and entropic differences between the isoforms in both binding processes. A structural comparison suggests that a variation in the conformation of the loop C−D, induced by mutation Asp/Gly, could be responsible for the differences in ligand-binding energetics. While recognition of lauric acid was entropically driven, recognition of sodium dodecyl sulfate was both entropically and enthalpically driven, confirming the key role of the ligand polar moiety. Because of a more favorable enthalpy, the dimerization equilibrium constant of βlgB was larger than that of βlgA at room temperature, while the two dimers became similarly stable at 35 °C. The isoforms exchanged the same number of structural water molecules and protons and shared similar stereochemistry at the dimer interface. MD simulations revealed that the subunits of both variants become more flexible upon dimer formation. It is hypothesized that a larger increase of βlgA mobility could account for the dimerization energetic differences observed.

Random changes in the genomic sequences that modify the primary structure of proteins provide the raw material with which natural evolution sculpts living organisms. In the last years, considerable progress has been achieved in understanding the connections between mutations and changes in the physicochemical and functional properties of proteins (*1*). Nevertheless, further research is still required to expand fully our ability to modify properties of natural proteins or to create *de novo* ones. In this sense, the study of natural protein isoforms is a subject of major interest, as they carry not only meaningful information on the relationship between structural and energetic properties but also on the functional context in which those mutations have been selected (*2*, *3*).

[†]This work was supported in part by DGAPA, UNAM (PAPIIT, Grant IN204609) and CONACyT (Grant 47097).

*To whom correspondence should be addressed. Phone: +52 55 56 22 44 24. Fax: +52 55 56 16 22 03. E-mail: egarciah@unam.mx.

[1]Abbreviations: βlg, bovine β-lactoglobulin; βlgA, βlg variant A; βlgB, βlg variant B; LA, lauric or dodecanoic acid; SDS, sodium dodecyl sulfate; K_b, equilibrium binding constant; *n*, binding stoichiometry; ΔH_b, binding enthalpy; ΔG_b, binding free energy of Gibbs, ΔS_b, binding entropy; K_D, equilibrium dimerization constant; ΔH_D, dimerization enthalpy; ΔG_b, dimerization free energy of Gibbs, ΔS_b, dimerization entropy; ΔC_{pb}, dimerization heat capacity; ITC, isothermal titration calorimetry; IDC, isothermal dilution calorimetry; ΔN_W, number of structural water molecules exchanged; ΔN_{H+}, number of protons exchanged; ΔH_{ion}, buffer ionization enthalpy; rmsd, root-mean-square deviation; RMSF, root-mean-squate fluctuation per residue; ΔA, surface area change; $\Delta C_{p\Delta A}$, desolvation heat capacity; ΔC_{pH2O}, heat capacity change of water molecule sequestering; ΔC_{pT}, total calculated heat capacity dimerization ($= \Delta C_{p\Delta A} + \Delta C_{pH2O}$); MD, molecular dynamics; NMR, nuclear magnetic resonance.

Bovine β-lactoglobulin (βlg)[1] is a prominent member of the lipocalin family, a large group of proteins involved in the transport of small hydrophobic molecules. βlg has nine β-strands (labeled βA to βI) and a three-turn α-helix (Hα) located between βH and βI. Eight of the β-strands (βA to βH) form a β-barrel sandwich with a central cavity, usually referred to as "calyx", which constitutes the main binding site of the protein. Loops A−B, C−D, E−F, and G−H flank the entrance of the cavity, while loops B−C, D−E, and F−G close the opposite side of the β-barrel (*4*). X-ray crystallography data have recently confirmed the existence of a secondary binding site, located on a solvent-exposed hydrophobic patch composed of Hα and βI residues (*5*). In spite of the numerous biophysical studies carried out on this relatively small protein (162 residues), it is still an intriguing case of study. βlg shows a complex conformational behavior. Unfolding studies have revealed the existence of a number of kinetic and equilibrium intermediates (*6*, *7*). Furthermore, this lipocalin represents an emblematic example of a β-sheet protein with a predominantly α-helical intermediate in its folding pathway (*8*, *9*). Above pH 3.5, the protein tends to self-associate (*10*). Between pH 6 and 8, it undergoes a number of conformational changes that collectively are known as the "Tanford transition" (*11*, *12*). This transition, characterized by an overall expansion of the molecule, modifies the conformation of the loop E−F. Under acidic conditions, the loop adopts a conformation that closes the entrance of the cavity, while at neutral and basic conditions, it folds back to expose the interior of the cavity. Thus, this loop seems to serve as a lid for controlling the access of ligands to the calyx.

Published on Web 11/30/2010

Several variants of βlg have been isolated from cow's milk. Among them, variants A (βlgA) and B (βlgB) are the most abundant. These variants differ only in two sites of the polypeptide chain: at the fully solvent-exposed position 64, Asp in βlgA is replaced by Gly in βlgB, and at position 118, immersed in the hydrophobic core of the molecule, Val in βlgA is changed by Ala in βlgB. With the pursuit of a careful comparison of structural properties, two laboratories have independently reported the X-ray structures of the isoforms under matched crystallization conditions. Qin et al. (*13*) crystallized the two variants at a nominal pH of 7.1 (PDB codes 1bsy and 1bsq for βlgA and βlgB dimers, respectively), while Oliveira et al. (*14*) used a nominal pH of 7.9 (PDB codes 1qg5 and 1b8e for βlgA and βlgB dimers, respectively). Small structural differences in the vicinity of the two mutations were reported in both studies. Replacement of Val to Ala at position 118 creates a void space in the core of the protein (~40 Å^3), which has been confirmed through pressure-induced unfolding studies (*15*). Furthermore, distinct conformations of the loop C−D (residues 60−69) were observed, which seem to arise from variations in the local electrostatic potential induced by the mutation Asp/Gly at position 64 (*16*). In spite of these relatively modest structural differences, the mutations significantly modify the physicochemical properties of βlg, including solubility (*17*), isoelectric point (*18*), structural mobility (*19*), dimerization and ligand-recognition energetics (*20*), and susceptibility to temperature, chaotropic agents (*21*), hydrostatic-pressure (*15*), and proteolysis (*22*). Some of these differences are of significant industrial interest, as they affect milk processing.

The ligand-binding capacity of βlg has been studied extensively in the past, mainly using spectroscopic techniques (*20*). The protein is able to recognize a wide variety of hydrophobic ligands, with binding constants (K_b) ranging from 10^2 to 10^8 M^{-1}. However, the number of studies dealing with the simultaneous characterization of the two major variants is still scarce. Furthermore, only K_b values obtained at a single temperature have been reported. In the present study, we have characterized the association of βlgA and βlgB to lauric (dodecanoic) acid (LA) by using high-precision isothermal titration calorimetry (ITC). This ligand was chosen since it was found to be the longest saturated fatty acid with solubility high enough to perform reliable calorimetric measurements. Furthermore, the binding of each variant to sodium dodecyl sulfate (SDS) was measured, with the aim of assessing the energetic importance of the ligand's polar tail in the interaction. βlgA and βlgB also show distinct self-association behaviors. While βlgB forms dimers, βlgA is able to octamerize between pH 3.5 and 5.5 (*18*). Furthermore, the dimer of βlgB is more stable than that of βlgA (*23*), though no systematic comparison of the energetic contributions responsible for this difference has been carried out. In a previous study, the dimerization energetics of βlgA was characterized calorimetrically at neutral pH (*24*). A structural-energetic analysis, in which the occurrence of coupled equilibria was taken into account, led to the conclusion that water sequestering has a major energetic role in the formation of the βlgA homodimer. In the present study, we have performed a similar characterization of βlgB and compared the homodimerization energetics of both variants.

MATERIALS AND METHODS

Materials. All chemicals, including bovine βlg variants A (L7880) and B (L8005) were from Sigma Chemical Co. Experiments were performed at pH 7.0 in a 0.05 M buffer phosphate solution supplemented with 0.1 M NaCl, unless otherwise stated. βlg was dissolved into the buffer solution and diafiltrated extensively in an Amicon stirred cell through polyethersulfone ultrafiltration discs. Protein concentration (MW = 18.2 kDa and 18.4 for βlgA and βlgB, respectively) was determined spectrophotometrically ($A_{0.1\%}^{280nm}$ = 0.97).

Isothermal Titration Calorimetry. The association of βlg variants to LA or SDS were measured calorimetrically using a VP-ITC instrument (MicroCal, Inc.). To reduce artifacts related to ligand self-aggregation, the minimal reactant concentrations were looked for that allowed performing reliable calorimetric measurements. Accordingly, all titration measurements were performed using a βlg monomer concentration of ~13 μM. The concentration of LA in the calorimetric syringe was 0.3 mM, which is significantly smaller than its critical micelle concentration (CMC = 1 mM). Nevertheless, the use of LA concentrations of up to 0.6 mM yielded similar results for the binding parameters. For titrations with SDS, a ligand concentration of 0.3 mM was used (CMC = 8.2 mM). The titration schedule consisted of 25−30 consecutive injections of 10 μL, with a 6 min interval between injections. The dilution heat of the ligand was obtained by adding it to a buffer solution under conditions identical to those used with the protein solution. The binding constant (K_b), enthalpy change (ΔH_b), and stoichiometry (n) were determined by the nonlinear fitting of normalized titration data using an identical and independent binding site model:

$$Q = \frac{nM_t\Delta H_b V_0}{2}\left[1+\frac{X_t}{nM_t}+\frac{1}{nK_bM_t} - \sqrt{\left(1+\frac{X_t}{nM_t}+\frac{1}{nK_bM_t}\right)^2-\frac{4X_t}{nM_t}}\right] \quad (1)$$

where Q is the normalized heat evolved per mole of ligand, after correction for dilution heats of the ligand, V_o is the working volume of cell, and X_t and M_t are the ligand and macromolecule concentrations, respectively.

Isothermal Dilution Calorimetry. The dissociation of the βlgB homodimer was characterized using isothermal dilution calorimetry (IDC). Stepwise additions of small aliquots of a solution of high protein concentration (typically 1.3 mM of monomer) were applied into the calorimetric reaction cell loaded with buffer solution. According to a simple dimer dissociation model (*25*), the heat measured upon addition of the ith injection of volume dV_i into the cell calorimeter would be

$$q_i = \Delta H_{disc}[P_2]_{syr}\,dV_i - \Delta H_{disc}\left([P_2]_i - [P_2]_{i-1}\right)\left(V_0+\frac{dV_i}{2}\right) \quad (2)$$

where ΔH_{disc} is the dissociation enthalpy of the dimer, and $[P]$ and $[P_2]$ are the molar concentrations of the free monomer and dimer, respectively. The dimer concentration in the reaction cell $[P_2]_i$ and the syringe $[P_2]_{syr}$ are in turn related to the corresponding equivalent monomer concentrations $[P_T]$ through the dissociation constant:

$$[P_T] = [P]+2[P_2] = K_{disc}{}^{1/2}[P_2]^{1/2}+2[P_2] \quad (3)$$

where K_{disc} is the equilibrium dissociation constant. ΔH_{disc} and K_{disc} were determined through a nonlinear regression fitting of eqs 2 and 3.

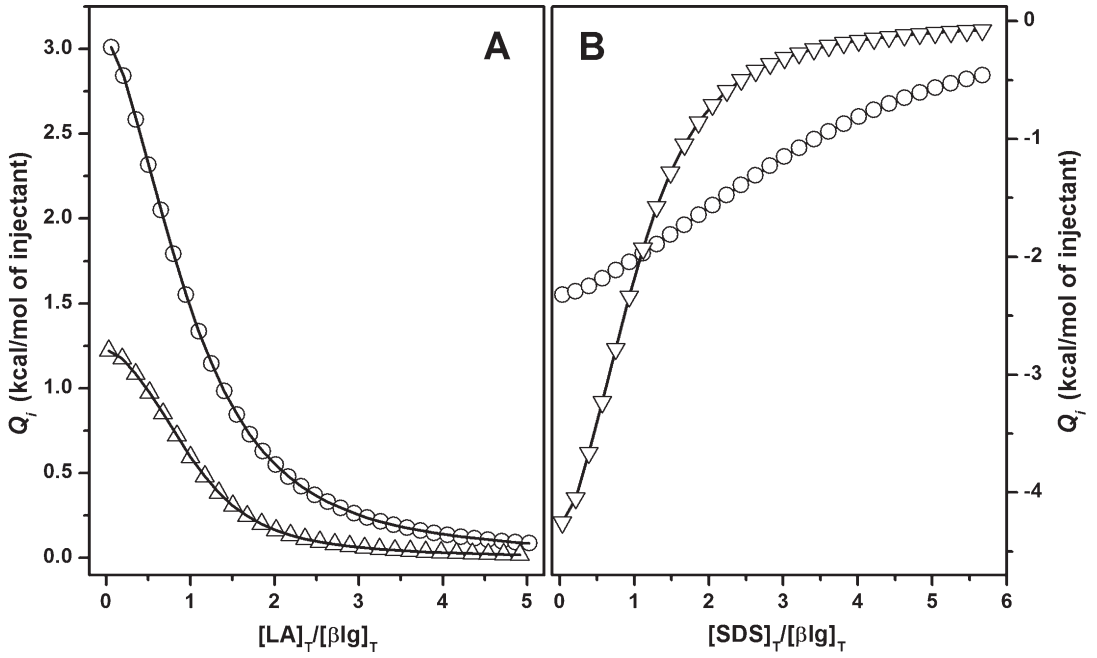

FIGURE 1: Isothermal titration calorimetry of lauric acid (A) and SDS (B) binding to βlgA (○) and βlgB (△,▽). In total, 35 5 μL aliquots of ligand (typically 0.3 mM) were injected into 1.42 mL of protein (13 μM of monomer). All experiments were conducted at pH 7.0, in a 0.05 M phosphates buffer, 0.1 M NaCl, and run in triplicate. The solid lines are the best fittings of a single site binding model to the experimental data.

Proton exchange was measured calorimetrically by conducting IDC experiments with buffers of different ionization enthalpy, ΔH_{ion}. The measured dissociation enthalpy, $\Delta H_{disc,obs}$, will vary as a function of the number of protons exchanged, ΔN_{H+}:

$$\Delta H_{disc,obs} = \Delta N_H + \Delta H_{ion} + \Delta H_{disc,b} \quad (4)$$

where $\Delta H_{disc,b}$ is the dissociation enthalpy free of buffer protonation effects. Measurements were carried out at 25 °C using buffers of quite different ΔH_{ion} (phosphate, ΔH_{ion} = 0.9 kcal mol^{-1}; bis-tris, ΔH_{ion} = 6.8 kcal mol^{-1}; tris, ΔH_{ion} = 11.3 kcal mol^{-1}).

Osmotic stress studies using nonionic osmolytes were conducted to measure hydration effects coupled to dimer formation (*24*). The number of water molecules that are not accessible to the osmolyte (ΔN_W) can be estimated from the dependence of the equilibrium constant on the osmolality of the solution, [osmol] (*26*):

$$\Delta N_W = -55.6 \frac{\partial \ln K}{\partial [\text{osmol}]} \quad (5)$$

Equation 5 assumes that no direct interaction between the cosolute and the protein takes place. Previously, it was shown that there is no interaction of βlgA with sucrose or acetamide (*24*). This last agent was used in experiments with βlgB.

Changes in Solvent-Accessible Surface Area. Surface area calculations were carried out with the NACCSESS program (S. J. Hubbard, J. M. Thornton, NACCESS. Computer program, Department of Biochemistry and Molecular Biology, University College, London, 1993) using a probe radius of 1.4 Å and a slice width of 0.1 Å. Changes in solvent-accessible surface areas (ΔA) were estimated from the difference between the complex and the sum of the free molecules.

Molecular Dynamics Simulations. The quality (bond lengths and angles, side chain planarity, atom chirality, Ramachandran analysis, packing quality, hydrogen bond positions, etc.) of the X-ray structures of the complexes of βlgA with Br-dodecanoic acid (PDB 1bso) and βlgB with palmitic acid (PDB 1bo0) and of the ligand-free dimers of βlgA (PDB 1bsy) and βlgB (PDB 1bsq) were checked with the WHAT IF Web interface (*27*). All MD simulations were performed in explicit solvent using a periodic truncated octahedral box by using the GROMACS simulation suite and the OPLS all-atom force field as described elsewhere (*24*).

RESULTS AND DISCUSSION

Ligand-Binding Energetics. Figure 1A shows the binding isotherms obtained for the titration of each βlg variant with LA at 35 °C, pH 7.0, using a protein concentration of 13 μM. Under these experimental conditions, both βlg variants are predominantly monomeric (see below). The isotherms were fitted satisfactorily using a single binding site model, yielding a stoichiometry of 1:1. Therefore, under the conditions used in this study, no evidence was observed for the binding of the fatty acid to the external secondary binding site. βlgB binds to LA with a 2-fold higher affinity in relation to βlgA (Table 1). This dissimilarity is due to the fact that although βlgA associates to the fatty acid gaining more degrees of freedom, it undergoes an even larger enthalpy increase compared to βlgB. The stronger affinity of βlgB for LA is consistent with previous noncalorimetric results. Spector and Fletcher (*28*), using equilibrium dialysis, found K_b = 52 000 M^{-1} for βlgA (pH 7.4, 37 °C), while Frapin et al. (*29*), using titration fluorimetry, obtained K_b = 1 430 000 M^{-1} (pH 7.0, 20 °C) for βlgB. The affinity difference between the two variants determined from these studies is larger than that obtained in the present study, a discrepancy that may be related in part to the use of different techniques and somewhat dissimilar experimental conditions.

LA and SDS differ from each other in the polar moiety, while they share the same aliphatic chain. Since SDS also binds into the βlg calyx (*30*, *31*), it can be used to gain insights into the importance of the ligand's polar head in the interaction.

Table 1: Energetics of LA and SDS Recognition by βlg Variants A and B[a]

ligand	variant	n^b	K_b $M^{-1} \times 10^{-5}$	ΔG_b kcal mol^{-1}	ΔH_b kcal mol^{-1}	$T\Delta S_b$ kcal mol^{-1}
LA	βlgA	0.94 ± 0.04	1.88 ± 0.08	−7.45 ± 0.20	4.58 ± 0.06	12.06 ± 0.18
	βlgB	0.99 ± 0.01	3.70 ± 0.02	−7.85 ± 0.16	1.56 ± 0.04	9.41 ± 0.30
SDS	βlgA	0.94 ± 0.02	1.07 ± 0.02	−6.98 ± 0.11	−2.52 ± 0.02	4.46 ± 0.09
	βlgB	0.98 ± 0.01	5.79 ± 0.06	−8.00 ± 0.09	−4.20 ± 0.01	3.81 ± 0.01

[a]Measurements were perfomed at pH 7.0 in a 0.05 M phosphates buffer, 0.1 M NaCl, at 35 and 30 °C for LA and SDS, respectively. Values for each entry are the mean of three independent experiments. [b]Ligand bound per monomer of protein.

Measurements for this ligand are reported at 30 °C (Figure 1B), since titration of βlgA at 35 °C yielded heat signals that were too small, precluding a reliable analysis of the data. The corresponding binding parameters are shown in Table 1. For each variant, 1 mol of SDS is bound per mol of protein monomer, with an affinity similar to that for LA. The K_b value obtained herein for βlgB is similar to that obtained previously using equilibrium dialysis ($K_b = 3.1 \times 10^5$ M^{-1}, pH 7.5 (*32*), and somewhat smaller than that determined fluorimetrically ($K_b = 4.35 \times 10^6$ M^{-1}, 20 °C (*33*)). At variance with that observed for LA, SDS recognition is both enthalpically and entropically driven. Furthermore, the entropy gain is considerably smaller with SDS. These results indicate that the ligand's polar group plays a major role in the interaction with βlg, a molecular feature difficult to disclose if only considering binding constant values at a single temperature. Rowshan et al. (*34*) found that the formation of the βlgB−SDS complex is more exothermic than that of βglA, in agreement with data in Table 1. In contrast, Taheri-Kafrani et al. (*35*) reported that βglA binds endothermically to SDS at pH 6.7. However, SDS concentrations above the CMC were used in both studies, and no binding parameters were reported. In an earlier thermometric study, Kresheck et al. (*36*) reported that the βlgB−SDS interaction is exothermic, finding values significantly more negative than those in Table 1, while binding constants were not determined.

Structural-Based Analysis of Ligand Binding. Qin et al. (*16*) solved the structure of βlgA bound to Br-dodecanoic acid. Shortly after, Wu et al. (*37*) reported the structure of the βlgB−palmitic acid complex. Both fatty acid-bound structures were obtained near neutral pH, with similar resolutions. We used these structures for modeling the two variants in complex with lauric acid by simply eliminating the extra ligand atoms in the Br-dodecanoic and palmitic acids. Figure 2A shows the overlapped structures of the variants in these complexes. Clearly, the two structures are very similar, showing an overall rmsd of 0.7 Å. However, a closer inspection reveals small, though plausibly significant, conformational differences. Table 2 shows distances between selected ligand−protein and protein−protein atom pairs. It can be seen that residues at positions 64 and 118 lie far away from the binding site (> 7 Å from the closest ligand atoms; see also Figure 2C), implying that the effects on the binding energetics of mutations at these positions must be indirect.

Residue 64 is located in the middle of the loop C−D, which flanks the entrance of the protein's binding site (Figure 2D). As shown in Figure 3A, the triad of residues Glu^{62}, Asn^{63}, and Asp/Gly^{64} exhibit largely different ϕ and/or ψ dihedral angle values in the two variants. Significant differences in the main-chain conformation of the loop C−D are also seen in the ligand-free structures of the isoforms (*13*). The reason for this conformational difference seems to be related to the presence of Asp^{64} in βlgA, which induces a rearrangement of the loop C−D in order to minimize electrostatic repulsions with nearby residues Glu^{62} and Glu^{65} (*13*). As a result, the contact pattern inside the loop and of the protein with the ligand differs significantly between the two variants (Figure 2D). In βlgA, the carbonyl group of Glu^{62} is fully exposed to the solvent, while in βlgB it is pointing toward the interior of the loop, forming a hydrogen bond with the main chain's amide group of Glu^{65}. In turn, the side chain of Glu^{62} in βlgB interacts simultaneously with Lys^{60} and Lys^{69}, while these two basic residues form electrostatic bridges with the carboxyl group of LA. In contrast, this electrostatic bonding network is not seen in βlgA. In this variant, Glu^{62} is moved away from the ligand, losing its contact with Lys^{60}. Furthermore, the interaction between the carboxylate of LA and Lys^{69} is disrupted, since this last residue is displaced in order to preserve its interaction with Glu^{62}. Overall, the larger number of contacts with the polar group of LA in βlgB may explain, at least in part, the less unfavorable binding enthalpy observed for this variant in relation to that observed for βlgA. In turn, it is conceivable that the formation of a more extensive hydrogen bonding network elicits a larger stiffening of the complex, a picture that is consistent with the less favorable ligand-binding entropy observed for βlgB.

To further explore the conformational dissimilarities between βlgA and βlgB, molecular dynamics simulations were carried out to determine the temporal course of the interactions of LA with Lys^{60} and Lys^{69}. Figure 3B shows the fraction of time during the simulation in which the carboxylic moiety of LA establishes interaction with none (0), one (1), or simultaneously the two lysine residues (2). In both variants, most of the time there are no ligand−protein hydrogen bonds. This picture is consistent with NMR results obtained for the binding of βlgB to ^{13}C-enriched palmitic acid, indicating that the ligand carboxylate shows a larger mobility compared with the mobility of atoms at the aliphatic tail (*38*). Yet, the MD simulations suggest that the hydrogen bonds formed with the fatty acid are more lasting and cooperative in βlgB than in βlgA.

A clear indication that the Asp/Gly mutation is implicated in the ligand-binding differences between βlgA and βlgB is the distinct recognition behavior observed with SDS. In both variants, ΔH_b is largely improved upon SDS binding (becoming an exothermic process), while ΔS_b is less favorable in relation to LA binding. Presumably, the larger size and number of hydrogen bond acceptors of the sulfate group facilitates a more extensive interaction of SDS with the protein. It is worthy to note that the differences in ΔH_b and ΔS_b between the βlg variants decrease considerably with SDS as the ligand (Table 1). In this case, the entropy gain is almost the same in βlgA and βlgB ($\Delta(T\Delta S_b) = 0.7$ kcal mol^{-1} for SDS vs 2.6 kcal mol^{-1} for LA), suggesting that both variants undergo a similar loss of structural flexibility. In contrast, the difference in the binding enthalpy is somewhat larger ($\Delta(\Delta H_b) = 1.7$ kcal mol^{-1}), suggesting that electrostatic effects that arise due to the presence of Asp^{64} are also considerable

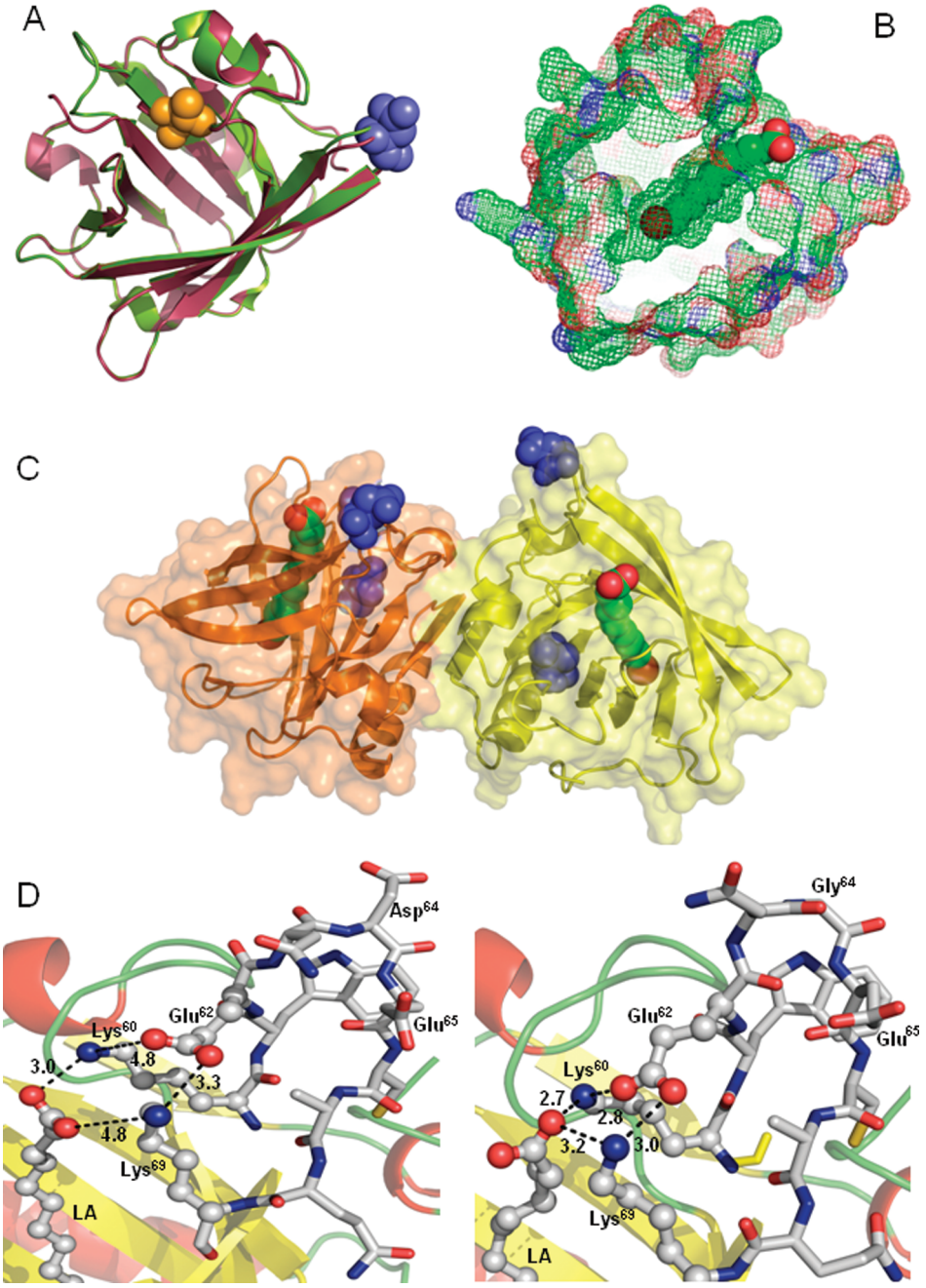

FIGURE 2: Structural aspects of βlg variants: (A) superposition of the X-ray structures of βlgA and βlgB, (B) perspective of the binding cavity of βlg, (C) βlgA dimer. Positions 64th (solvent exposed) and 118th (buried) in the polypeptide chain are in white spheres, while the ligand molecule is shown in CPK colored spheres. (D) Conformation of the loop C−D and its interaction with the fatty acid in the βlgA (left) and βlgB (right) structures. Numbers correspond to the distance (in angstroms) between atomic centers.

Table 2: Distances between Selected Ligand−Protein and Protein−Protein Atom Pairs in the LA-Bounded Structures of βlg Variants

	βlgA (1bso.pdb)	βlgB (1bo0.pdb)
ligand−protein	LA(O1)−D^{64}(N): **13.9**	LA(O1)−G^{64}(N): **12.0**
	LA(O2)−K^{60}(NZ): **3.1**	LA(O2)−K^{60}(NZ): **2.7**
	LA(O1)−K^{69}(NZ): **4.8**	LA(O1)−K^{69}(NZ): **3.2**
	LA(C6)−V^{118}(CB): **7.9**	LA(C6)−A^{118}(CB): **7.8**
	LA(C6)−V^{118}(CG1): **7.5**	
	LA(C4)−L^{39}(CD2): **5.4**	LA(C6)−L^{39}(CD1): **4.2**
protein−protein (intracatenary)	V^{118}(CB)−L^{39}(CD2): **3.6**	A^{118}(CB)−L^{39}(CB): **4.1**
	V^{118}(CG1)−R^{40}(N): **6.4**	A^{118}(CB)−R^{40}(N): **6.9**
	D^{64}(CA)−A^{34}(CB): **11.7**	G^{64}(CA)−A^{34}(CB): **9.8**

in the interaction with SDS. Thus, it seems that subtle differences in the configuration of the protein's residues interacting with the ligand's polar group are responsible for the dissimilarities observed in the recognition of LA.

Although residue 118 is also not seen interacting directly with the ligand in the X-ray structures of the two fatty acid-βlg complexes, it does contact Leu^{39}, which in turn forms part of the protein's binding cavity. As shown in Table 2, Leu^{39} establishes a van der Waals contact with Val^{118} in βlgA that is not seen with Ala^{118} in βlgB. In turn, Leu^{39} in βlgB is significantly displaced toward the LA molecule, making a contact with the aliphatic chain of the ligand. In contrast, this contact is not seen in the βlgA complex. Thus, it cannot be ruled out that the

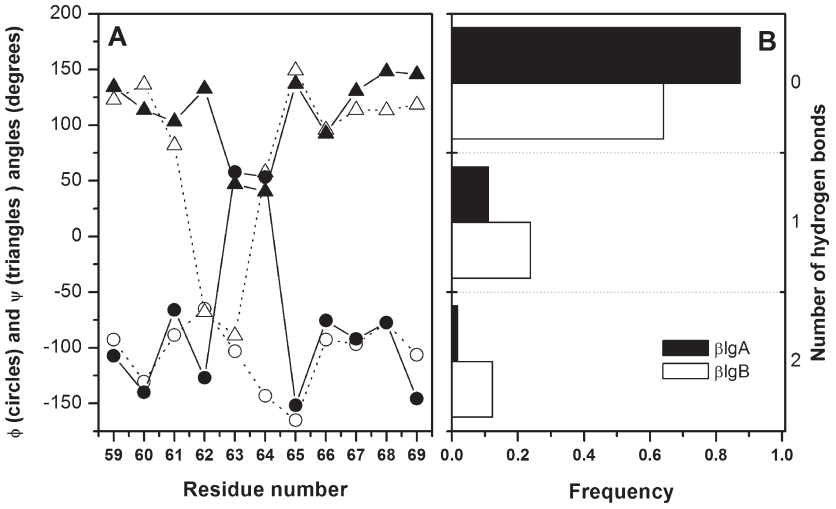

FIGURE 3: (A) Comparison of ϕ (○,●) and ψ (△,▲) values of residues forming the loop C−D in βlgA (○,△) and βlgB (●,▲). (B) Fraction of time during a 50 ns-long MD simulation in which the carboxylic moiety of LA establishes interaction with none (0), one (1), or simultaneously both Lys^{60} and t Lys^{69} (depicted in Figure 2D), in βlgA (solid bars) and βlgB (open bars).

mutation Val/Ala(118), occurring in the core of the protein, could also be contributing to the different ligand-binding behaviors of the βlg variants.

"Classical" vs "Nonclassical" Hydrophobic Effect in βlg−Ligand Interactions. Analysis of transfer data of model compounds has led to the classical picture whereby the hydrophobic effect is entropically driven, while the enthalpic contribution is marginally favorable or unfavorable. Nevertheless, it has been observed in an increasing number of cases that the recognition of hydrophobic ligands by proteins may be characterized by a so-called nonclassical hydrophobic effect (*39*). In these cases, the process is enthalpically driven, while the binding entropy may even be largely unfavorable. Frequently, the coordination of the ligand's polar moiety, occurring at the bottom of the low-dielectric binding cavity, has been implicated as the main source of the favorable binding enthalpy (*40*−*44*). For instance, pheromonal ligands bind to mouse major urinary protein (MUP-1) via water-mediated hydrogen bonding networks with internal polar residues. Mutations that disrupt these interactions diminish significantly the favorable binding enthalpy, while the binding entropy becomes favorable (*45*).

Classical hydrophobic-like signatures were observed for the recognition of LA by the two βlg variants. This is not surprising, since around 90% of the contact areas between the ligand and the protein are hydrophobic. Conversely, nonclassical hydrophobic-like features were exhibited in SDS recognition. Displacement titrations of LA-prebound βlg with SDS demonstrate that the two ligands compete for the same binding site (*30*, *31*), indicating that SDS association also involves extensive apolar-to-apolar contacts between the ligand and the protein. Thus, the switch from a classical to a nonclassical hydrophobic behavior in βlg's recognition is primarily determined by the nature of the ligand's polar moiety. It is worth to note that, at variance with other proteins showing a nonclassical hydrophobic effect, the ligand−protein polar-to-polar interactions in βlg complexes occur at the entrance of the binding site, with a high degree of exposure to the solvent. Thus, a low dielectric environment is not obligatory for the development of exothermic interactions between charged groups.

Energetics of Self-Association. The homodimerization energetics of βlgB was characterized calorimetrically at neutral pH by means of IDC, under the same conditions used previously for βlgA (*24*). As an example of the calorimetric results, Figure 4A shows the dissociation isotherm obtained at 25 °C, which was well fitted using a simple dimer dissociation model. Table 3 summarizes calorimetric results obtained in the temperature range of 15−35 °C, expressed in terms of dimer formation (i.e., K_D, ΔG_D, ΔH_D, and ΔS_D). Self-association was enthalpically driven throughout the temperature range spanned. In contrast, the process was entropically favored at the lower and opposed at the higher temperatures sampled, implying that the maximum stability of the dimer occurs at room temperature. Linear regression analysis of ΔH_D vs. temperature yields a ΔC_{pD} value of -459 ± 9 cal mol^{-1} K^{-1}.

The exchange of small molecules coupled to the formation of the βlgB dimer was also quantified calorimetrically. Proton exchange was determined by performing measurements in buffer solutions of varying ionization enthalpy (ΔH_{ion}). Figure 4B (○) shows the observed dimerization enthalpy (ΔH_{obs}) obtained in three different buffer solutions. The slope of this plot (eq 4) is consistent with a marginal uptake of protons, $\Delta N_{H+} = 0.24 \pm 0.02$. In contrast, calorimetric measurements performed under osmotic stress conditions reveal a strong dependence of K_D on the cosolute osmolality (Figure 4B, ●), indicating the sequestering of a large number of water molecules ($\Delta N_W = 36 \pm 2$) upon dimer formation (eq 5).

Figure 5 compares the thermodynamic formation signatures of βlgA and βlgB homodimers. It was established 4 decades ago via sedimentation equilibrium that βlgB exhibits a K_D 3-fold larger than that of βlgA (*23*). Our calorimetric measurements are consistent with that picture, though a smaller difference between the two variants was observed (K_D ~50% higher for βlgB). Considerable differences in ΔH_D and $T\Delta S_D$ were observed between the two variants. Formation of the βlgB homodimer is enthalpically more favored ($\Delta\Delta H_D = -2.3$ kcal mol^{-1}), while it loses a larger number of degrees of freedom ($\Delta(T\Delta S_D) = -1.9$ kcal mol^{-1}) than βlgA. The more exothermic formation of the βlgB dimer implies a higher thermal dependence of the equilibrium constant for this complex. As a consequence, the βlgB dimer is seen to be more stable than the βlgA dimer at low temperatures, while the two dimers become equally stable around 35 °C (see also Table 1 in ref *24*). As shown in Figure 5, the ΔC_{pD} value of βlgB is slightly less negative ($\Delta\Delta C_{pD} = 36$ cal mol^{-1} K^{-1}) than

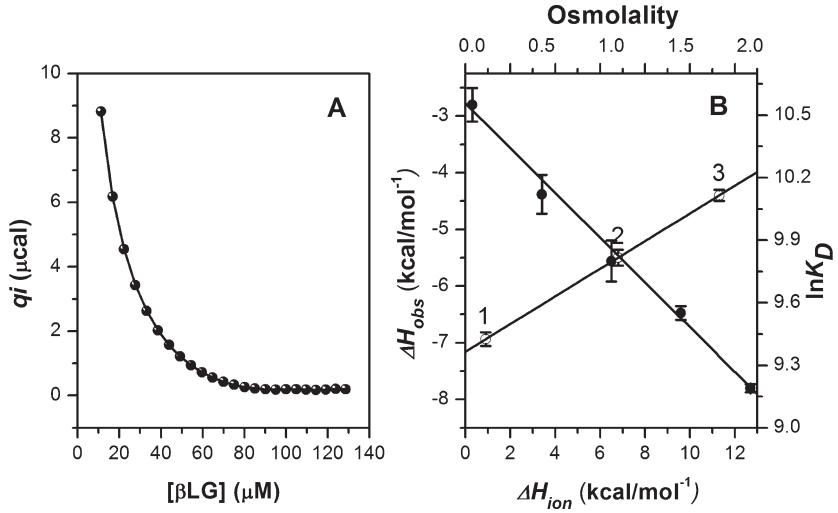

FIGURE 4: (A) Calorimetric dissociation isotherm of βlgB, obtained at 25 °C, pH 7.0, in a 0.05 M phosphates buffer, 0.1 M NaCl. The solid line represents the best fitting of a simple dimer dissociation model to the calorimetric data. (B) Calorimetric determinations of protons (○) and structural water molecules (●) exchanged upon formation of the βlgB homodimer. For the evaluation of the number of protons exchanged (eq 4), three buffer systems with different ionization enthalpies were used (1) phosphate, $\Delta H_{ion} = 0.9$ kcal mol^{-1}; (2) bis-tris, $\Delta H_{ion} = 6.8$ kcal mol^{-1}; and (3) tris, $\Delta H_{ion} = 11.3$ kcal mol^{-1}. For the evaluation of the number of water molecules exchanged (eq 5), acetamide was used as the stress agent. All experiments were in triplicate, at 25 °C, pH 7.0, in a 0.05 M phosphates buffer, 0.1 M NaCl. See the Materials and Methods for details.

Table 3: Energetics of βlgB Homodimer Formation Measured Calorimetrically[a]

temperature °C	K_D M^{-1} × 10^{-3}	ΔG_D kcal mol^{-1}	ΔH_D kcal mol^{-1}	$-T\Delta S_D$ kcal mol^{-1}
15	83.4 ± 0.7	−6.49 ± 0.05	−2.98 ± 0.16	−3.51 ± 0.07
20	69.2 ± 0.5	−6.49 ± 0.01	−5.77 ± 0.53	−0.72 ± 0.07
25	46.2 ± 0.3	−6.36 ± 0.06	−6.94 ± 0.24	+0.58 ± 0.04
30	28.8 ± 0.2	−6.19 ± 0.04	−9.86 ± 0.15	+3.68 ± 0.05
35	18.0 ± 0.1	−6.00 ± 0.05	−12.30 ± 0.35	+6.30 ± 0.12

[a]Measurements were performed at pH 7.0 in a 0.05 M phosphates buffer, 0.1 M NaCl. Values for each entry are the mean of three independent experiments.

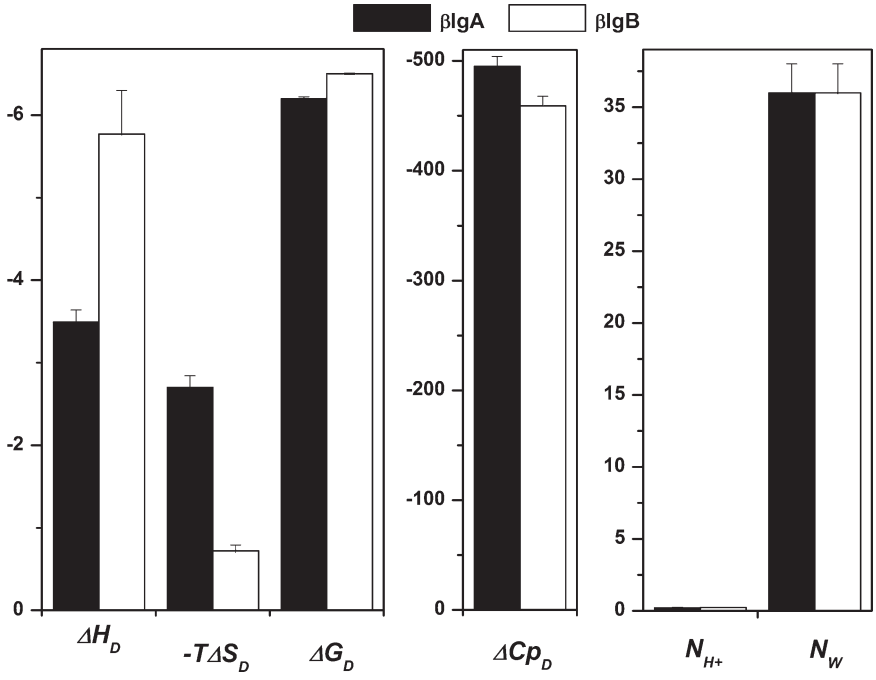

FIGURE 5: Thermodynamic signatures determined calorimetrically for the formation of βlgA (solid bars) and βlgB (open bars) homodimers. ΔH_D, $T\Delta S_D$, and ΔG_D (at 20 °C) are in kilocalories mole^{-1}, ΔC_{pD} is in calories mole^{-1} Kelvin^{-1}.

that of βlgA. This difference, though small, is beyond experimental uncertainty. Figure 5 also shows that the two variants exchange the same numbers of protons and structural water molecules upon dimer formation.

Table 4: Hydrogen Bonding at the Dimer Interfaces of βlg Variants

subunit1−subunit2	βlgA[a] (1bsy)	βlgB[a] (1bsq)	βlgA[b] (1qg5)	βlgB[b] (1b8e)	βlgA-B[c] (1beb)
D^{33}(OD1)−R^{40}(NH1)	4.4	4.9	3.4	**3.1**	**2.9**
D^{33}(OD1)−R^{40}(NH2)	4.7	5.0	3.9	**2.6**	**2.9**
R^{40}(NH2)−D^{33}(OD1)	5.7	4.9	3.9	**3.1**	**2.9**
R^{40}(NH1)−D^{33}(OD1)	4.4	5.0	3.4	**2.6**	**3.0**
H^{146}(ND1)−S^{150}(OG/O)	3.6	3.7	3.7	4.0	4.3
H^{146}(O)−S^{150}(N)	**2.9**	**2.9**	**3.0**	**3.0**	**2.9**
R^{148}(N)−R^{148}(O)	**2.8**	**2.7**	**2.9**	**2.9**	**3.0**
R^{148}(O)−R^{148}(N)	**2.8**	**2.7**	**3.0**	**2.9**	**3.0**
S^{150}(N)−H^{146}(O)	**2.9**	**2.9**	**3.0**	**3.0**	**3.0**
S^{150}(OG/O)−H^{146}(ND1)	3.6	3.7	3.7	4.0	**3.0**

[a]Crystallized under matched conditions, at a nominal pH of 7.3 (*13*). [b]Crystallized under matched conditions, at a nominal pH of 7.9 (*14*). [c]Crystallized at a nominal pH of 6.5, as a mixture of the two isoforms (*47*).

Table 5: Surface Area Changes and Structural-Based Calculations of Heat Capacity Changes for βlgA and βlgB Homodimers

PDB code	variant	ΔA_{ap} Å^2	ΔA_p Å^2	$\Delta C_{p\Delta A}$ cal mol^{-1} K^{-1}	ΔC_{pT}[a] cal mol^{-1} K^{-1}
1bsy[b]	βlgA	−548	−380	−148	−443
1bsq[b]	βlgB	−527	−397	−134	−429
1qg5[c]	βlgA	−480	−428	−105	−400
1be8[c]	βlgB	−481	−460	−97	−392

[a]Desolvation heat capacity ($\Delta C_{p\Delta A}$) was calculated according to eq 6. The total calculated heat capacity change (ΔC_{pT}) is the sum of $\Delta C_{p\Delta A}$ plus the change rising from the freezing of 36 water molecules (ΔC_{pH2O}), considering a contribution of −8.2 cal mol^{-1} K^{-1} per water molecule (*24*). [b]Crystallized under matched conditions, at a nominal pH of 7.3 (*13*). [c]Crystallized under matched conditions, at a nominal pH of 7.9 (*14*).

Structural-Based Analysis of Self-Association. Residues 64 and 118 are distant from the dimer interface (> 7 Å), implying that the mutations occurring at these positions, as in the case of ligand binding, exert an indirect effect on the dimer energetics (Figure 2B). It has been proposed that the two extra methyl groups of Val^{118} induce a displacement of residues 37−40 in relation to their positions observed in the presence of Ala^{118}, a variation that perturbs the interaction at the dimer interface, thus affecting the monomer−dimer equilibrium (*46*). To check this suggestion, we compared two pairs of X-ray structures of βlgA and βlgB which have been solved under similar conditions (*13*, *14*). Table 4 lists the donor−acceptor atom pairs that have been suggested to participate in the stabilization of the βlg dimer interface (*47*), as well as the respective atomic distances observed in the two pair of dimers. In all these structures, the corresponding space group has a monomer in the asymmetric unit, i.e., the intersubunit bonding could be significantly affected by the space group. Table 4 also shows distances observed in a crystal structure obtained at a nominal pH of 6.5, for which the dimer is in the asymmetric unit (PDB 1beb (*47*)); however, in this case a mixture of the two isoforms (βlgA−B) was crystallized. Clearly, no consensus picture about hydrogen bonding differences between the two βlg homodimers can be derived from the comparative inspection of data in Table 4.

Table 5 shows the interfacial surface areas (ΔA) calculated from the two sets of crystal structures of βlg variants. Isoforms obtained at the same pH show basically the same amounts of ΔA, while larger differences are observed among dimers obtained at different pH values. Table 5 also shows calculations for the desolvation heat capacity change ($\Delta C_{p\Delta A}$) based on the surface area model:

$$\Delta C_{p_{\Delta A}} = -0.26\Delta A_p + 0.45\Delta A_{ap} \quad (6)$$

where ΔA_p and ΔA_{ap} stand for changes in the solvent-accessibility of polar (oxygen plus nitrogen) and apolar (carbon plus sulfur) surface areas, respectively. Parameters for this model have units of calories mole^{-1} Kelvin^{-1} angstrom^{-2} and were obtained from the analysis of the transfer of cyclic dipeptides from the solid state to an aqueous solution (*48*). Thus, they have proven successful in estimating heat capacity changes of protein folding and protein binding processes where the desolvation of the contacting areas is the predominant contribution (*49*, *50*). As shown in Table 5, for both variants $\Delta C_{p\Delta A}$ accounts for just a fraction of the experimental ΔC_{pD}. Previously, it was shown that the incorporation of water molecules into the dimer interface largely affects the energetics of βlgA self-association (*24*). In contrast, no significant contributions from subunit conformational rearrangements or exchange of protons or counterions take place. As stated above, osmotic stress measurements reveal that the two homodimers incorporate the same number of structural water molecules ($\Delta N_W = 36$). Considering the value of −8.2 cal mol^{-1} K^{-1} for the freezing of a single water molecule, the heat capacity change associated to the sequestering of 36 water molecules (ΔC_{pH2O}) would amount to −295 cal mol^{-1} K^{-1}. The sum of this last value with that calculated for $\Delta C_{p\Delta A}$ yields estimations ($\Delta C_{pT} = \Delta C_{p\Delta A} + \Delta C_{pH2O}$) close to those determined calorimetrically (Table 5). Nevertheless, it is interesting to note that, regardless of the structure or the variant considered, an underestimation of the thermodynamic parameter is observed, suggesting the probable occurrence of additional molecular processes.

βlg Structural Dynamics. Large changes in the structural mobility of a protein can have significant effects on its association energetics (*51*). It is well-known that βlg shows large structural fluctuations in relation to other globular proteins (*52*). This flexibility is due in part to the presence of a central binding cavity, which makes βlg lack a compact hydrophobic core. Furthermore, it has been postulated that significant "breathing" movements are necessary to allow the insertion of long ligands into the calyx (Figure 2B). Contrasting pictures regarding the differences in the

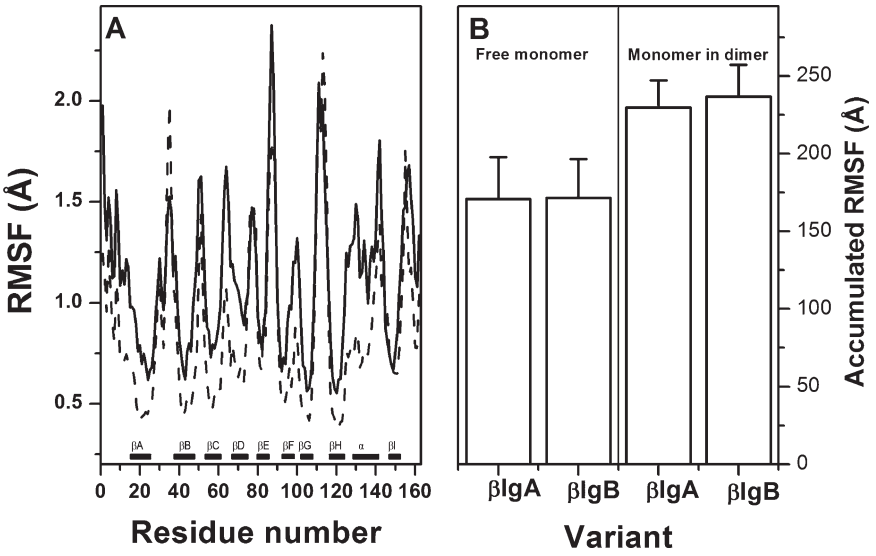

FIGURE 6: Structural dynamics of βlg variants. (A) Root mean squared fluctuation (RMSF) per residue of the free (– – –) and dimerized (—) subunit of βlgA obtained over the last 40 ns of a 50 ns-long DM simulation. (B) Accumulated RMSF values, calculated by summing the RMSF values of each line in panel A. Simulations were conducted in explicit solvent, using GROMACS simulation suite and the OPLS all-atom force field. Results shown are the average of four independent runs.

structural dynamics of βlgA and βlgB have been put forward. For instance, analyses of the temperature factors of structures obtained under similar crystallization conditions have led to the conclusion that variant A (*14*) or variant B (*13*) is more flexible than the other isoform. Few studies have been carried out to address the dynamics differences in solution of βlg isoforms. The distinct reactivity of the thiol group of the buried Cys^{121} has been taken as evidence of a larger structural flexibility of the βlgB isoform. In contrast, an analysis of the hydrogen−deuterium exchange rates determined via infrared spectroscopy showed that βlgA undergoes faster structural fluctuations (*19*). This last finding agrees with the 5-fold larger tryptic hydrolysis rates of βlgA over βlgB observed under different temperature and pH conditions (*22*).

It is worthy to recall that βlgA shows a more favorable entropy contribution both in self-association and ligand-binding processes (Tables 1 and 3). It is tempting to hypothesize that this feature could be related to an increased structural flexibility of this isoform. Regarding the ligand-recognition process, it has been observed that although palmitate-binding reduces the proteolytic rates of βlgA and βlgB, implying an overall reduction of the structural flexibility in both variants, the stiffening effect is more pronounced in βlgB (*22*). On the other hand, Goto and coworkers, using heteronuclear NMR, demonstrated that fatty-acid binding increases the mobility of many residues lying at the entrance of the binding cavity, mainly in the β-strand D and the loops E−F and G−H (*52*, *53*). A similar structural loosening accompanies the Tanford transition (*54*), indicating that this behavior is a conspicuous characteristic of βlg. Considering, on the one hand, the evidence of that upon ligand binding, the residues forming the entrance of the βlg cavity are prone to increase their structural flexibility, and, on the other, that a weaker interaction seems to be established between βlgA and the LA's polar group (Figures 2 and 3), the larger ΔS_b observed for this variant with respect to βlgB could be rationalized in terms of a larger increase in the conformational dynamics of the open end of its β-barrel calyx.

In relation to the self-association entropy change, in a study based on two-dimensional infrared and Raman correlation spectroscopy, Jung et al. (*55*) observed secondary structural changes of βlg that depend on protein concentration. Analyzing the signals of the amide III region, the authors proposed that the increase of protein concentration perturbs the unordered and ordered secondary elements, inducing an expansion of the molecule. Furthermore, it was suggested that this expansion is accompanied by water penetration into the protein. Clearly, this last suggestion is in agreement with the osmotic stress results obtained for the two βlg variants (Figure 5). To explore whether significant changes in the structural dynamics occur upon dimer formation, 50 ns-long MD simulations were carried on both variants. Figure 6A shows the RMSF for the free (dotted line) and dimerized (solid line) subunits of βlgA. As expected, the loops showed the largest fluctuations both in the dimer and the free monomer, while the movements of the β-strands and the α-helix were more restricted. The RMSF profiles in Figure 6A resemble closely the ^{15}N spin−lattice (T_1) relaxation times obtained using NMR spectroscopy by Uhrínová et al. (*56*) for the βlgA's free monomer at acid conditions. Figure 6B shows the accumulated RMSF for the two βlg variants. Values correspond to the average of four independent MD runs with the standard deviations shown as bar errors. Clearly, in both variants a significant increase in mobility accompanies the formation of the dimer, in agreement with the spectroscopic evidence provided by Jung et al. (*55*). Four independent MD runs were carried out for the monomer and dimer of each variant (see the Supporting Information), while a long time was sampled in the simulations. In spite of that, no significant differences in the dynamic changes of βlgA and βlgB were observed, although it is recognized that the uncertainties inherent to current MD simulation protocols are still considerable (*58*). Nevertheless, considering the differences in the formation of the two dimers, it seems that just a somewhat larger increase of βlgA flexibility would be enough to explain the more favorable dimerization entropy observed experimentally for this variant.

CONCLUDING REMARKS

Although βlg is one of the most studied globular proteins, its complex behavior in solution makes it a challenging case of study

in modern physicochemical and biochemical research. In this study, we performed a detailed characterization of the ligand binding energetics of βlgA and βlgB, the most prevalent variants in cow's milk. Furthermore, the self-recognition energetics of βlgB was calorimetrically measured, as previously done for βlgA (*24*). The two amino-acid substitutions that distinguish βlgA and βlgB have a significant impact on the energetics of both ligand binding and self-recognition processes. Since these substitutions occur at positions far away from the intermolecular contact zones, their effects on the binding energetics must be indirect, perturbing proximal and perhaps distal regions in the protein molecule. In the case of ligand binding, structural and MD simulation data suggest that a rearrangement of the loop C−D, induced by substitution of Asp/Gly at position 64th, yields a different interaction pattern of the protein with the polar moiety of the ligand. Calorimetric measurements reveal that, as previously shown for βlgA, the homodimerization energetics of βlgB is highly influenced by water sequestering. Furthermore, spectroscopic and computational results indicate that the subunits of the two variants become more flexible upon dimer formation. The increase in backbone mobility as a means to improve entropically the binding affinity in biomolecular recognition phenomena has been documented for an increasing number of protein complexes in recent years (*57*−*59*), including the recognition of hydrophobic molecules by the major urinary protein (MUP-I), a relative of βlg (*44*). However, further work is still needed to unveil the molecular bases of such a behavior.

ACKNOWLEDGMENT

M.B. and M.C.P.T. received fellowships from CONACyT and DGAPA. Computer support and CPU time for the simulations were facilitated by DGSCA. We thank M. in S. Virginia Gómez Vidales for her unvaluable assistance in the ITC experiments.

SUPPORTING INFORMATION AVAILABLE

Figure showing individual RMSF results obtained from the different MD runs for the dimers and the free monomers of both βlgA and βlgB. This material is available free of charge via the Internet at http://pubs.acs.org.

REFERENCES

1. Siegel, J. B., Zanghellini, A., Lovick, H. M., Kiss, G., Lambert, A. R., St. Clair, J. L., Gallaher, J. L., Hilvert, D., Gelb, M. H., Stoddard, B. L., Houk, K. N., Michael, F. E., and Baker, D. (2010) Computational design of an enzyme catalyst for a stereoselective bimolecular Diels-Alder reaction. *Science 329*, 309–313.
2. Allali-Hassani, A., Wasney, G. A., Chau, I., Hong, B. S., Senisterra, G., Loppnau, P., Shu, Z., Moult, J., Edwards, A. M., Arrowsmith, C. H., Park, H. W., Schapira, M., and Vedad, M. (2009) A survey of proteins encoded by non-synonymous single nucleotide polymorphisms reveals a significant fraction with altered stability and activity. *Biochem. J. 424*, 15–26.
3. Costas, M., Rodríguez-Larrea, D., De Maria, L., Borchert, T. V., Gómez-Puyou and, A., and Sanchez-Ruiz, J. M. (2009) Between-species variation in the kinetic stability of TIM proteins linked to solvation-barrier free energies. *J. Mol. Biol. 385*, 924–937.
4. Kontopidis, G., Holt, C., and Sawyer, L. (2004) β-Lactoglobulin: binding properties, structure, and function. *J. Dairy Sci. 87*, 785–796.
5. Yang, M.-C., Guan, H.-H., Liu, M.-Y., Lin, Y.-H., Yang, J.-M., Chen, W.-L., Chen, C.-J., and Mao, S. J. T. (2008) Crystal structure of a secondary vitamin D_3 binding site of milk β-lactoglobulin. *Proteins: Struct., Funct., Bioinf. 71*, 1197–1210.
6. Hamada, D., and Goto, Y. (1997) The equilibrium intermediate of β-lactoglobulin with non-native α-helical structure. *J. Mol. Biol. 269*, 479–487.
7. García-Hernández, E., Hernández-Arana, A., Zubillaga, R. A., and Rojo-Domínguez, A. (1998) Thermodynamic and spectroscopic evidence for a complex denaturation mechanism of bovine β-lactoglobulin A. *Biochem. Mol. Biol. Int. 45*, 761–768.
8. Kuwajima, K., Yamaya, H., and Sugai, S. (1996) The burst-phase intermediate in the refolding of β-lactoglobulin studied by stopped-flow circular dichroism and absorption spectroscopy. *J. Mol. Biol. 264*, 806–822.
9. García-Hernández, E., Villena-Iribe, R., Hernández-Santoyo, A., and Rodríguez-Romero, A. (1999) Desnaturalización térmica de la β-lactoglobulina en soluciones agua-etanol. *Rev. Latinoamericana Quím. 27*, 58–63.
10. McKenzie, H. A., and Sawyer, W. H. (1967) Effect of pH on β-lactoglobulins. *Nature 214*, 1101–1104.
11. Qin, B. Y., Bewley, M. C., Creamer, L. K., Baker, H. M., Baker, E. N., and Jameson, G. B. (1998) Structural basis of the Tanford transition of bovine β-lactoglobulin. *Biochemistry 37*, 14014–14023.
12. Sakurai, K., and Goto, Y. (2007) Principal component analysis of the pH-dependent conformational transitions of bovine β-lactoglobulin monitored by heteronuclear NMR. *Proc. Natl. Acad. Sci. U.S.A. 104*, 15346–15351.
13. Qin, B. Y., Bewley, M. C., Creamer, L. K., Baker, E. N., and Jameson, G. B. (1999) Functional implications of structural differences between variants A and B of bovine β-lactoglobulin. *Protein Sci. 8*, 75–83.
14. Oliveira, K. M. G., Valente-Mesquita, V. L., Botelho, M. M., Sawyer, L., Ferreira, S. T., and Polikarpov, I. (2001) Crystal structures of bovine β-lactoglobulin in the orthorhombic space group C2221. Structural differences between genetic variants A and B and features of the Tanford transition. *Eur. J. Biochem. 268*, 477–483.
15. Botelho, M. M., Valente-Mesquita, V. L., Oliveira, K. M., Polikarpov, I., and Ferreira, S. T. (2000) Pressure denaturation of β-lactoglobulin: different stabilities of isoforms A and B, and an investigation of the Tanford transition. *Eur. J. Biochem. 267*, 2235–2241.
16. Qin, B. Y., Creamer, L. K., Baker, H. M., and Jameson, G. B. (1998) 12-Bromododecanoic acid binds inside the calyx of bovine β-lactoglobulin. *FEBS Lett. 438*, 272–278.
17. Treece, J. M., Sheinson, R. S., and McMeekin, T. L. (1964) The solubilities of β-lactoglobulins A, B and AB. *Arch. Biochem. Biophys. 108*, 99–108.
18. Bash, J. J., and Timasheff, S. N. (1967) Hydrogen ion equilibria of the genetic variants of bovine β-lactoglobulin. *Arch. Biochem. Biophys. 118*, 37–47.
19. Dong, A., Matsuura, J., Allison, S. D., Chrisman, E., Manning, M. C., and Carpenter, J. F. (1996) Infrared and circular dichroism spectroscopic characterization of structural differences between β-lactoglobulin A and B. *Biochemistry 35*, 1450–1457.
20. Sawyer, L. (2003) β-lactoglobulin, in Advanced Dairy Chemistry (Fox, P. F., McSweeney, P. L. H., Eds.) 3rd ed., Vol. 1, pp 319−386, Kluwer Academic/Plenum Publishers, New York.
21. Boye, J. I., Ma, C. Y., and Ismail, A. (2004) Thermal stability of β-lactoglobulins A and B: effect of SDS, urea, cysteine and N-ethylmaleimide. *J. Dairy Res. 71*, 207–215.
22. Creamer, L. K., Nilsson, H. C., Paulsson, M. A., Coker, C. J., Hill, J. P., and Jiménez-Flores, R. (2004) Effect of genetic variation on the tryptic hydrolysis of bovine β-lactoglobulin A, B, and C. *J. Dairy Sci. 87*, 4023–4032.
23. Zimmerman, J. K., Barlow, G. H., and Klotz, I. M. (1970) Dissociation of β-lactoglobulin near neutral pH. *Arch. Biophys. Biochem. 138*, 101–109.
24. Bello, M., Pérez-Hernández, G., Fernández-Velasco, D. A., Arreguín-Espinosa, R., and García-Hernández, E. (2008) Energetics of protein homodimerization: effects of water sequestering on the formation of β-lactoglobulin dimer. *Proteins: Struct., Funct., Bioinf. 70*, 1475–1487.
25. Velázquez-Campoy, A, Leavitt, S. A., and Freire, E. (2004) Characterization of protein-protein interactions by isothermal titration calorimetry. *Methods Mol. Biol. 261*, 35–54.
26. Parsegian, V. A., Rand, R. P., and Rau, D. C. (1995) Macromolecules and water: probing with osmotic stress. *Methods Enzymol. 259*, 43–94.
27. Vriend, G. (1990) WHAT IF: A molecular modelling and drug design program. *J. Mol. Graph. 8*, 52–56.
28. Spector, A. A., and Fletcher, J. E. (1970) Binding of long chain fatty acids to β-lactoglobulin. *Lipids 5*, 403–411.
29. Frapin, D., Dufour, E., and Hartlé, T. (1993) Probing the fatty-acid binding site of β-lactoglobulins. *J. Prot. Chem. 12*, 443–449.
30. McMeekin, T. L., Polis, B. D., DellaMonica, E . S., and Custer, J. H. (1949) Crystalline compound of β-lactoglobulin with dodecyl sulfate. *J. Am. Chem. Soc. 71*, 3606–3609.

31. Creamer, L. K. (1995) Effect of sodium dodecyl sulfate and palmitic acid on the equilibrium unfolding of bovine β-lactoglobulin. *Biochemistry 34*, 7170–7176.
32. Ray, A., Chatterjee, R. (1967) Interactions of β-lactoglobulins with large organic ions, in Conformation of Biopolymers (Ramachandran, G. N., Ed.) Vol. 1, pp 235−52, Academic Press, London.
33. Lamiot, E., Dufour, E., and Haertlé, T. (1994) Insect sex pheromone binding by bovine β-lactoglobulin. *J. Agric. Food Chem. 42*, 695–699.
34. Rowshan, H., Bordbar, A. K., and Moosavi-Movahedi, A. A. (1996) The thermodynamic stability of the different forms of β-lactoglobulin (A and B) to sodium *n*-dodecyl sulphate. *Thermochim. Acta 285*, 221–229.
35. Taheri-Kafrani, A., Bordbar, A.-K., Mousavi, S. H.-A., and Haertlé, T. (2008) β-lactoglobulin structure and retinol binding changes in presence of anionic and neutral detergents. *J. Agric. Food Chem. 56*, 7528–7534.
36. Kresheck, G. C., Hargraves, W. A., and Mann, D. C. (1977) Thermometric titration studies of ligand binding to macromolecules. Sodium dodecyl sulfate to β-lactoglobulin. *J. Phys. Chem. 81*, 532–537.
37. Wu, S. Y., Perez, M. D., Puyol, P., and Sawyer, L. (1999) β-lactoglobulin binds palmitate within its central cavity. *J. Biol. Chem. 274*, 170–174.
38. Ragona, L., Fogolari, F., Zetta, L., Pérez, M. D., Puyol, P., de Kruif, K., Löhr, F., Röterjans, H., and Molinari, H. (2000) Bovine β-lactoglobulin: interaction studies with palmitic acid. *Protein Sci. 9*, 1247–56.
39. Syme, N. R., Dennis, C., Phillips, S. E. V., and Homans, S. W. (2007) Origin of heat capacity changes in a "nonclassical" hydrophobic interaction. *ChemBioChem 8*, 1509–151.
40. Færgeman, N. J., Sigurskjold, B. W., Kragelund, B. B., Andersen, K. V., and Knudsen, J. (1996) Thermodynamics of ligand binding to acyl-coenzyme A binding protein studied by titration calorimetry. *Biochemistry 35*, 14118–26.
41. Nielsen, A. D., Borch, K., and Westh, P. (2000) Thermochemistry of the specific binding of C12 surfactants to bovine serum albumin. *Biochim. Biophys. Acta 1479*, 321–331.
42. Wolfrum, C., Börchers, T., Sacchettini, J. C., and Spener, F. (2000) Binding of fatty acids and peroxisome proliferators to orthologous fatty acid binding proteins from human, murine, and bovine liver. *Biochemistry 39*, 1469–1474.
43. Hanhoff, T., Lücke, C, and Spener, F. (2002) Insights into binding of fatty acids by fatty acid binding proteins. *Mol. Cell. Biochem. 239*, 45–54.
44. Bingham, R. J., Findlay, J. B. C., Hsieh, S.-Y., Kalverda, A. P., Kjellberg, A., Perazzolo, C., Phillips, S. E. V., Seshadri, K., Trinh, C. H., Turnbull, W. B., Bodenhausen, G., and Homans, S. W. (2004) Thermodynamics of binding of 2-methoxy-3-isopropylpyrazine and 2-methoxy-3-isobutylpyrazine to the major urinary protein. *J. Am. Chem. Soc. 126*, 1675–1681.
45. Sharrow, S. D., Edmonds, K. A., Goodman, M. A., Novotny, M. V., and Stone, M. J. (2005) Thermodynamic consequences of disrupting a water-mediated hydrogen bond network in a protein:pheromone complex. *Protein Sci. 14*, 249–256.
46. Bewley, M. C., Qin, B. Y., Hameson, G. B., Sawyer, L., Baker, E. N. (1997) Bovine β-lactoglobulin and its variants: a three-dimensional structural perspective, in International Dairy Federation. Milk Protein Polymorphism, Issue 9702, pp 100−109, International Dairy Federation, Brussels, Belgium.
47. Brownlow, S., Cabral, J. H. M., Cooper, R., Flower, D. R., Yewdall, S. J., Polikarpov, I., North, A. C. T., and Sawyer, L. (1997) Bovine β-lactoglobulin at 1.8 Å resolution - still an enigmatic lipocalin. *Structure 5*, 481–495.
48. Murphy, K. P., and Freire, E. (1992) Thermodynamics of structural stability and cooperative folding behavior in proteins. *Adv. Protein Chem. 43*, 313–361.
49. García-Hernández, E., Zubillaga, R. A., Chavelas-Adame, E. A., Vázquez-Contreras, E., Rojo-Domínguez, A., and Costas, M. (2003) Structural energetics of protein−carbohydrate interactions. Insights derived from the study of lysozyme binding to its natural saccharide inhibitors. *Protein Sci. 12*, 135–142.
50. Ladbury, J. E., and Williams, M. A. (2004) The extended interface: measuring non-local effects in biomolecular interactions. *Curr. Opin. Struct. Biol. 14*, 562–569.
51. Tidor, B., and Karplus, M. (1994) The contribution of vibrational entropy to molecular association. The dimerization of insulin. *J. Mol. Biol. 238*, 405–414.
52. Sakurai, K., Konuma, T., Yagi, M., and Goto, Y. (2009) Structural dynamics and folding of β-lactoglobulin probed by heteronuclear NMR. *Biochim. Biophys. Acta 1790*, 527–537.
53. Konuma, T., Sakurai, K., and Goto, Y. (2007) Promiscuous binding of ligands by β-lactoglobulin involves hydrophobic interactions and plasticity. *J. Mol. Biol. 368*, 209–218.
54. Sakurai, K., and Goto, Y. (2006) Dynamics and mechanism of the Tanford transition of bovine β-lactoglobulin studied using heteronuclear NMR spectroscopy. *J. Mol. Biol. 356*, 483–496.
55. Jung, Y. M., Czarnik-Matusewicz, B., and Ozaki, Y. (2000) Two-dimensional infrared, two-dimensional Raman, and two-dimensional infrared and Raman heterospectral correlation studies of secondary structure of β-lactoglobulin in buffer solutions. *J. Phys. Chem. B 104*, 7812–7817.
56. Uhrínová, S., Smith, M. H., Jameson, G. B., Uhrín, D., Sawyer, L., and Barlow, P. N. (2000) Structural changes accompanying pH-induced dissociation of the β-Lactoglobulin dimer. *Biochemistry 39*, 3565–3574.
57. Fayos, R., Melacini, G., Newlon, M., Burns, L., Scott, J., and Jennings, P. (2003) Induction of flexibility through protein-protein interactions. *J. Biol. Chem. 278*, 18581–18587.
58. Grünberg, R., Nilges, M., and Leckner, J. (2006) Flexibility and conformational entropy in protein-protein binding. *Structure 14*, 683–693.
59. MacRaild, C. A., Hernández Daranas, A., Bronowska, A., and Homans., S. W. (2007) Global changes in local protein dynamics reduce the entropic cost of carbohydrate binding in the arabinose-binding protein. *J. Mol. Biol. 368*, 822–832.